Effects of the solid-liquid interface in filter cake formation and consolidation

EFFECTS OF THE SOLID-LIQUID INTERFACE IN FILTER CAKE FORMATION AND CONSOLIDATION

R.J. Wakeman, E.S. Tarleton (e.s.tarleton@lboro.ac.uk) and M.N. Sabri
Separation Processes Centre, University of Exeter, Exeter, UK.

ABSTRACT

New data are reported on the formation of filter cakes. Cake formation data are analysed through two consecutive mechanisms, filtration and consolidation. Process design parameters for each mechanism are obtained from the models which might allow calculations to be made from small scale experiments. The magnitude and dependence of the constitutive parameters on pressure, pH and surface charge, particle size and shape, and the nature of the particle-particle interactions are shown through the experimental results.

INTRODUCTION

In the literature there is a lot of data which reports the characteristics of solid/liquid filtration[1]. One of the drawbacks of these earlier experiments is that none report all the relevant data pertaining to the particles and their solution environment even though the particles may be fine enough for interfacial properties to dominate their behaviour; it is therefore not possible to know which properties of the mixture affect compression. There is similarly a considerable amount of data in the colloid science literature[2-4] which has generally been obtained using 'ideal' particles (such as latices). These latter works have given insight into the fundamental parameters, but have not yielded engineering data or pointed to design methodologies of practical significance.

This paper summarises some results obtained previously[5] to provide a wider understanding of the effects of fundamental properties on design data obtained for particulates which have industrial significance. Results from an experimental study of the compression of solid/liquid mixtures are reported; the mixtures have been characterised in respect of their particle size and shape, the surface charge on the particles and the resulting aggregation of the particulate phase, and the phase compositions of the mixture. The surface charge and state of aggregation are interpreted through the pH, although the relationships between electrophoretic mobility (and hence zeta potential) and pH were measured for each suspension studied.

EXPERIMENTAL APPROACH & PROCEDURE

Studies of intermolecular forces require the highest degree of cleanliness and care because of the unpredictable behaviour of impurities on the primary mechanism. A mild detergent solution was used to clean all equipment, which was then thoroughly rinsed with twice distilled water prior to the start of an experiment. The suspensions were prepared by dispersing the particles in twice distilled water ($2xH_2O$), shaken vigorously by a flask shaker, and the particles allowed to settle before any excess liquid was decanted off. This process of washing and decanting using twice distilled water was repeated until a constant solution conductivity was reached. The solids volume fraction was then adjusted to that required for the experiment, and the pH altered by the addition of HCl or NaOH. The pH was varied over as wide a range as the solid would allow without reaction taking place; in most instances this enabled experiments from around the point of zero charge to close to the charge maximum or minimum. The finer particle suspensions were prepared from coarse material by milling.

The particles used were anatase (supplied by Tioxide PLC), china clay (ECC International Ltd), calcite and hydromagnesite (BDH Chemicals Ltd). Their sizes were measured using a Malvern

Cite paper as: Wakeman R.J., Tarleton E.S. and Sabri M.N., 1992, Effects of the solid-liquid interface in filter cake formation and consolidation, *Proc. European Symposium on Solid-Liquid Separation*, Paper L16, 14 pp., Cologne, Germany.

Autosizer 2c or Coulter Counter as appropriate according to the size of the particles, and their zeta potentials was determined using a Malvern Zetasizer 2c. Their general shape was checked by scanning electron microscope examinations.

The particles used and their quantitative characteristics are summarised in Table 1. Apart from being of industrial interest the selection of the particles for study was also based on their relative properties, so that particles of differing shape, size and surface charge were used.

The filtration apparatus, illustrated in Figure 1, comprised an upright, polished stainless steel, cylinder mounted on a circular base. The cylinder had an internal bore of 43 mm and a height of 193 mm and was filled by suspension at the start of a test, so that different compact thicknesses were formed by starting the experiment with a different concentration of suspension. The base contained a 43 mm diameter recess into which a loosely fitting stainless steel sinter disc was inserted; this disc supported a porous membrane onto which the compact was deposited. A drain carried away liquid expelled from the solid/liquid mixture. A piston, actuated by a pneumatic cylinder, was used to force liquid from the cylinder. A load cell, mounted in the end of the piston was used to monitor the force exerted onto the suspension. This assembly is referred to as the piston press in the following.

During an experiment a rotary encoder measured the downward displacement of the piston, and enabled determination of the volume of liquid displaced from the cylinder (and hence calculation of the solids volume fraction of the mixture remaining in the cylinder). These measurements were checked by monitoring simultaneously the expelled liquid volume on a digital scale connected to a multichannel chart recorder. A timer, synchronised with the encoder, enabled the rate of piston movement to be evaluated.

The piston was driven by one of two pneumatic cylinders; the smaller allowed pressures in the range 0.3 to 3.5 MPa to be exerted on the solid/liquid mixture, and the larger capable of providing 6 to 40 MPa (the maximum pressure used was limited to 20 MPa by the installed load cell and the strength of the sintered disc). Each experiment was carried out at a constant pressure (as applied to the mixture).

RELEVANT THEORY

The theory used to analyse the experimental data[5,7] has been summarised elsewhere[5], and so only the final working relationships are given below. The filtration of a stable suspension is made up of two parts; an initial stage in which filtration to form a cake occurs, followed by a consolidation stage during which the bulk volume of the deposited cake is reduced. If the starting suspension is unstable, the combined processes of filtration and sedimentation are responsible for the initial stage. In the experiments reported here the initial stage was completed in a much shorter time than it took the suspension to sediment in a gravity field; the effects of sedimentation were therefore neglected in subsequent analyses.

Data are available from the piston press as the thickness of the solid/liquid mixture as a function of pressing time, and as the volume of liquid expressed as a function of time. These data can be converted one to the other, and serve to check that a material balance is preserved during the experiment and that there were no malfunctions of the measuring apparati. The thickness L of the solid/liquid mixture in the cylinder at any time is known and, using the mass fraction M_s, of solids in the press, the solids volume fraction ε_s can be calculated.

The ratio of the mass of wet compact per unit mass of dry compact m is related to the volume fraction of solids in the compact ε_s by:

Cite paper as: Wakeman R.J., Tarleton E.S. and Sabri M.N., 1992, Effects of the solid-liquid interface in filter cake formation and consolidation, *Proc. European Symposium on Solid-Liquid Separation*, Paper L16, 14 pp., Cologne, Germany.

$$m = 1 + \frac{\rho(1-\varepsilon_s)}{\rho_s \varepsilon_s} \qquad (1)$$

and the ratio of the mass of feed slurry to the mass of solids in the feed $1/s$ is obtained by applying equation (1) to the feed suspension.

The cake thickness at the transition from filtration to consolidation is obtained from:

$$L_1 = \left(\frac{m_1 - 1}{\rho} + \frac{1}{\rho_s} \right) \rho_s \omega_0 \qquad (2)$$

where m_1 is the ratio of the mass of wet compact to the mass of dry compact (M_{s1}^{-1}) at the end of the filtration period, and ω_0 is the volume of solids in the press per unit area. The value of m_1 cannot be measured experimentally during a test, and so is estimated from the known characteristics of constant pressure filtration. The transition from filtration to consolidation mechanisms occurs when the solid/liquid mixture has a thickness of L_1. On a plot of $-\Delta L/\Delta t^{0.5}$ against t, constant pressure filtration data should be represented by a horizontal line (it is better to use logarithmic scales for this plot so that data scatter does not hide the transition point). When the concentration of solids in the mixture exceeds a limiting value, the mixture passes into a semi-solid state and from thereon it is consolidated and the value of $-\Delta L/\Delta t^{0.5}$ decreases; at the end of the consolidation process it reaches a value of zero. It may sometimes take a long time for the true equilibrium to be established, and hence for the end of the process to be reached. The transition point for the mixture under test, L_1, is determined from the graph as the point where $-\Delta L/\Delta t^{0.5}$ starts to decrease rapidly.

Analysis of the First Stage: Cake Formation

The equation describing the filtration period is the conventional filtration equation:

$$\frac{1}{A}\frac{dV}{dt} = \frac{A\Delta p}{\mu(\alpha c V + AR)} \qquad (3)$$

However, the integrated form of this equation is generally more convenient to use as the expelled liquid data are usually collected as volumes rather than flow rates. The integrated form of equation (3) at constant pressure is

$$\frac{t - t_i}{V - V_i} = \frac{K_1}{2}(V + V_i) + K_2 \qquad (4)$$

where $K_1 = \alpha c\mu/A^2\Delta p$ and $K_2 = \mu R/A\Delta p$. Plotting the data from the filtration stage as $(t - t_i)/(V - V_i)$ against $(V + V_i)$ leads to a straight line from which the compact formation properties characterising the rate of the first stage of compression may be evaluated; when the start of filtration coincides with the start of the integration $t_i = V_i = 0$. The effective concentration of solids in the feed to be used in equations (3) and (4) is given by:

$$c = \frac{\rho s}{1 - ms}$$

where m is evaluated at the transition from slurry filtration to cake consolidation, i.e. $m = m_1$. A sample set of data are shown on Figure 2; compact formation is taking place over the first part of the plot, and the pronounced increase of the slope is seen where compact consolidation takes place.

Cite paper as: Wakeman R.J., Tarleton E.S. and Sabri M.N., 1992, Effects of the solid-liquid interface in filter cake formation and consolidation, *Proc. European Symposium on Solid-Liquid Separation*, Paper L16, 14 pp., Cologne, Germany.

Analysis of the Second Stage: Cake Consolidation

The consolidation period, $L < L_1$, is analysed through the use of an empirical relationship relating the consolidation ratio

$$U_c = \frac{L_1 - L}{L_1 - L_\infty} \tag{5}$$

to a dimensionless consolidation time T_c. A parametric expression has been developed[8] which approximates the solution to the Terzaghi[9,10] model to within 3%, and that relationship has been modified to[7]:

$$U_c = \frac{\sqrt{4T_c/\pi}}{\left(1+\left(4T_c/\pi\right)^v\right)^{1/2v}} \tag{6}$$

where v is the consolidation behaviour index which takes secondary consolidation effects into account. This equation takes no account of the effects of creep and the behaviour index was assigned a constant values of 2.85. The rationale for $v = 2.85$ was simply that it fitted the Terzaghi model equations, but experimental data suggest that $v > 2.85$ is a reality[5].

A value for C_e is obtained from the initial slope of the plot of U_c vs. $t_c^{0.5}$. For $T_c << 1$

$$U_c = \sqrt{\frac{4}{\pi}T_c} \tag{7}$$

and

$$K_e = \left(\text{slope}\right)^2 = \frac{4i^2C_e}{\pi\omega_0^2} \tag{8}$$

from which C_e is calculated. A plot of the experimental data shown in Figure 2 but for $L < L_1$, together with the fit of equation (6) to the data, is given in Figure 3. The agreement between theory and experiment shown here is typical of all the results which demonstrated consolidation behaviour.

EXPERIMENTAL RESULTS

Particle size has a major effect on compaction which becomes more difficult and more protracted as size is reduced; for example, 15 μm calcite particles in a 0.09 volume fraction suspension were fully compacted within 20 s whilst a 3 μm suspension required 2000 s under the same conditions. Only a few experiments were carried out with the coarser calcite particles, as clearly these are not a problem to compact and gravity settling made a significant contribution to the formation of the compact. As the particle size is decreased interparticle repulsive forces become appreciable compared with gravitational and imposed mechanical forces, and the permeability of the compact is lower. The final moisture content of the compact is affected to only a small extent by particle size provided the imposed force is sufficiently large to overcome the repulsive forces.

The effect of suspension concentration was to modify the rate of expression, with lower rates being found at higher concentrations. This is largely due to the more rapid formation of a thicker cake, causing the resistance to liquid flow to increase faster during the cake formation process. Lower

Cite paper as: Wakeman R.J., Tarleton E.S. and Sabri M.N., 1992, Effects of the solid-liquid interface in filter cake formation and consolidation, *Proc. European Symposium on Solid-Liquid Separation*, Paper L16, 14 pp., Cologne, Germany.

feed concentrations produced cakes with a higher voids ratio, but the latter was constant at feed solids volume fractions greater than ~0.1.

Compaction pressure was found to have a large effect on some suspensions, but a fairly minor one on others. In general terms higher pressures lead to the more rapid formation of more densely packed cakes, but such statements must be qualified by the magnitude of the surface charge on the particles. Two examples of the effects of pressure are shown in Figures 4 and 5. Figure 5 shows pressure affecting the rate of compaction to a much greater extent than it does the final packing density, whereas Figure 4 shows the converse with the final solids volume fraction being affected to a much greater extent than the rate of compaction. The reasons for these different behaviours lie with the range over which the interparticle forces extend. Hydromagnesite is a composite of $MgCO_3$, $Mg(OH)_2$ and water of hydration and the magnitude of the pressures existing between the particles at high separation distances (~300 nm at 0.4 volume fraction) presents a problem which might only be explained by (a) a double layer charge being given by the lattice charge of the mineral or (b) a thick layer of structured water over the particle surface. The diffuse double layer then originates at this distance from the surface. The lattice charge would need to correspond to a much higher surface potential than zeta potential measurements would suggest. It is difficult to reconcile the magnitude of the interparticle pressures observed with expectations from double layer theory when considering the hydromagnesite data.

Effects of pH on filtration were found to vary according to the magnitude of the surface charge on the particles. Calcite had a low zeta potential (< |20| mV) and the repulsive forces are correspondingly low. As might be expected, calcite data showed negligible effects of pH on either the rate of compaction or the final porosity of the cake. At the other extreme, the magnitude of the zeta potential of anatase (up to ~ |60| mV) caused marked changes in the rate of compaction, as shown on Figure 6. Most rapid filtration occurred at the point of zero charge, whereas at greater (either positive or negative) zeta potentials the rate was reduced. At the lower pH shown on Figure 6 the ionic strength is high, thereby causing suppression of the double layer and a reduction in the magnitude of the repulsive force. The effects of pH (through the double layer thickness) on the final packing density appeared to be small in comparison with the effects demonstrated by the surface of hydromagnesite.

It is interesting to note the different general shapes of the curves on Figure 6 in comparison with those on Figures 4 and 5. The extreme forms on Figures 4 axe indicative of a long period of cake consolidation, whereas those on Figure 6 occur when there is no contribution from the consolidation mechanism.

DISCUSSION OF RESULTS

Data shown on plots similar to Figures 5 and 6 can be replotted according to equation (4); Figure 7 shows an alternative plot for anatase suspensions. This plot also indicates the sharp transition from filtration to consolidation for the anatase data, compared with a more gradual change for the hydromagnesite. The gradient on the initial portion of these plots is proportional to the specific resistance per unit pressure difference ($\alpha/\Delta p$) of the deposit being formed; in all cases the gradient decreases less rapidly than the applied pressure increases, resulting in an increase of specific resistance with applied pressure.

Experimental data from the piston press were available in the form of the volume of filtrate (V) or the piston displacement as a function of time (t). From these data and the conditions of the experiment it was necessary to evaluate the specific cake resistance (α) during the filtration stage of the compression process, and the modified consolidation coefficient (C_e) and the behaviour index (v) during the consolidation stage. These are the factors to be used in any subsequent design calculations. The voids ratio (e) in equilibrium with the applied pressure gives a measure of the limiting packing density achievable at that pressure. From analyses of several compression

Cite paper as: Wakeman R.J., Tarleton E.S. and Sabri M.N., 1992, Effects of the solid-liquid interface in filter cake formation and consolidation, *Proc. European Symposium on Solid-Liquid Separation*, Paper L16, 14 pp., Cologne, Germany.

tests carried out at different pressures in the piston press, the parameters α and voids ratio can be plotted as functions of the applied pressure Δp. Useful expressions for these purposes are only valid over a specified pressure range and take the form:

$$\alpha = \alpha_0 p^n \tag{9}$$

$$e = e_0 - b \log p \tag{10}$$

where α_0, n, e_0 and b are coefficients of the solid/liquid system of interest, α is the specific resistance of the deposit formed during the filtration stage and e is the voids ratio of the cake at the end of the filtration process. Typical examples of the α vs. p relationships are shown on Figure 8, illustrating the decrease in permeability associated with higher applied pressures. The permeability similarly decreases when the particles are better dispersed; changing the pH of the china clay suspension from 2.9 ($\zeta \approx$ -15 mV) to 10.2 ($\zeta \approx$ -57 mV) increases the specific resistance by a factor of about one order of magnitude.

An example of the e vs. p relationship is shown on Figure 9. pH or surface charge appears to have no effect on the equilibrium voids ratio at these higher pressures. Reducing the particle size (at a constant pH) results in a higher equilibrium voids ratio. This is presumably a manifestation of the greater charge density around the surface of the finer particles.

The coefficients characterising the compression phase of the operation, C_e and v, are also known from the piston press results and may be represented by the equations:

$$C_e = C_{e0} p^v \tag{11}$$

$$v = \frac{4p}{\delta + p} \tag{12}$$

Coefficients arising from applications of the constitutive equations to the experimental data are summarised in Table 2. The limiting value of v at high pressures is 4 according to equation (12), but it is recognised that v is likely to be pressure dependent at lower applied pressures or when resisting forces between the particles are unusually high.

The data in Table 2 generally show the trends which might be anticipated, but there are also some unexpected results. With the exception of calcite the specific resistance increases and the compact voids ratio decreases with increasing pressure. Over the limited pressure range of the calcite tests there was not a detectable change in the compact permeability or specific resistance, in spite of a reduction of the voids ratio.

The less obvious results arise from consolidation of the anatase and hydromagnesite beds. For china clay the modified consolidation coefficient (C_e) increases with pressure, with a much increased sensitivity to pressure being observed at greater $|\zeta|$-potentials, but the consolidation behaviour index (v) was constant. However, for anatase both the modified consolidation coefficient and the consolidation behaviour index were found to be independent of pressure; a value of the packing density close to the limit measured at the end of the experiment was obtained whilst the filtration mechanism was effective, leaving little potential for further consolidation of the compact. The most curious result was the reduction of C_e with increasing pressure for hydromagnesite, together with the dependence of v on pressure.

The different behaviour of hydromagnesite requires further consideration, as it may be attributed to various causes. The shape of the hydromagnesite particle is similar to that of a calcite particle and not too dissimilar from that of an anatase particle, and the surface charge is similar to that at a

Cite paper as: Wakeman R.J., Tarleton E.S. and Sabri M.N., 1992, Effects of the solid-liquid interface in filter cake formation and consolidation, *Proc. European Symposium on Solid-Liquid Separation*, Paper L16, 14 pp., Cologne, Germany.

calcite surface. However, the size of the hydromagnesite particle is much greater than that of calcite or anatase and significant surface charge effects would not be expected to arise. A notable difference between the three particle systems is their solubility in cold water: anatase is insoluble, calcite has a solubility of 0.0014 g/100 ml, and hydromagnesite 0.04 g/100 ml. The solubility for hydromagnesite is greater than the corresponding solubility of either the carbonate (0.0106 g/100 ml) or hydroxide (0.0009 g/100 ml) in isolation, and could be expected to increase the electrolyte concentration near to the particle surfaces. If this led to a layer of structured liquid over the surface of the particle, it may explain why such anomalous results were obtained. To verify the precise reasons for these results will require considerably more research.

It is worth highlighting the effects of increasing the surface charge on the filtration process. Comparisons between the calcite and china clay data are particularly suitable for this: for calcite $\zeta \approx -16$ mV at pH 11.8, and for china clay $\zeta \approx -57$ mV at pH 10.2 and $\zeta \approx -15$ mV at pH 2.9. The effect of charge alone is seen by comparing the china clay data at pH's 10.2 and 2.9. The ultimate packing densities at the two pH's are not very different, as shown by the e_0 and b values on Table 2 and by Figure 9, but a higher surface charge considerably increases the resistance to compact formation, shown by the α_0 values in Table 2. The effect of higher surface charges slowing the kinetics of formation is also demonstrated clearly for an unwashed anatase on Figure 6. Effects of particle shape and at $\zeta \approx |15|$ mV are seen by comparing the anatase and china clay data at pH's 11.8 and 2.9 respectively; the calcite has lower resistances to compact formation and consolidation and the particles approach their ultimate packing density at only slightly lower pressures. The surface charge is more uniformly distributed around the more regularly shaped calcite than around the plate-like china clay particles whose packing can resemble the so-called 'house of cards' structure. A regular shape enables the fluid between the particles to act as a lubricant, resulting in the ability of the particles to pack closer to the ultimate value before the consolidation process occurs. Other things being equal, increasing the surface charge density around the particles leads to slower compaction by both the filtration and consolidation mechanisms.

Cakes formed from lower feed solids concentrations were formed only by the filtration mechanism, whereas cakes formed from higher concentration feeds are also subject to consolidation. Furthermore, there seems to be a minimum pressure needed before both mechanisms become effective in cake filtration.

CONCLUSIONS

The nature of the cake formation from fine particle suspensions is dependent on the applied pressure, pH and surface charge, particle size and shape, and the nature of the particle-particle interactions. The form of the filtration curves can vary widely, but they can all be analysed through the application of a two stage mechanism model. The two stages, which act consecutively, are the basic filtration and consolidation processes. Data have been presented for some selected solid/liquid systems to show how the compression characteristics change with the basic and fundamental properties of the solid/liquid mixture.

ACKNOWLEDGEMENTS

The authors wish to record their gratitude for receipt of grants from the Science & Engineering Research Council Specially Promoted Programme in Particulate Technology, those companies supporting the Industrial Research Consortium of the Separation Processes Centre at Exeter University, and the International Fine Particle Research Institute. The results presented here were obtained with assistance from those grants.

NOTATION

Cite paper as: Wakeman R.J., Tarleton E.S. and Sabri M.N., 1992, Effects of the solid-liquid interface in filter cake formation and consolidation, *Proc. European Symposium on Solid-Liquid Separation*, Paper L16, 14 pp., Cologne, Germany.

A cross-sectional area of compact (rn^2)
b coefficient in the voids ratio equation (10)
c effective concentration of solids in feed suspension (kg m^{-3})
C_e modified consolidation coefficient (m^2 s^{-1})
C_{e0} modified consolidation coefficient at Δp = 1 MPa
e voids ratio
e_0 voids ratio at Δp = 1 MPa
i number of drainage surfaces in the press
K_e = $4i^2C_e/\pi\omega_0^2$ (s^{-1})
K_1 = $\alpha c\mu/A^2\Delta p$ (s rn^{-6})
K_2 = $\mu R/A\Delta p$ (s m^{-3})
L thickness of solid/liquid mixture (m)
m ratio of mass of wet compact to mass of dry compact
M_s mass fraction of solids in the mixture
n index in the specific resistance equation (9)
p applied pressure (Pa or MPa)
Δp ≈ the applied pressure (Pa or MPa)
R resistance of the supporting medium (m^{-1})
s mass of solids per unit mass of slurry
t time (s)
t_c consolidation time (s)
T_c dimensionless consolidation time
U_c consolidation ratio defined by equation (5)
V volume of liquid expelled from the mixture (m^3)
$V(0)$ volume of mixture in the press at t = 0 (m^3)
x_{av} mean particle size (μm)

α specific resistance of the compact (m kg^{-1})
α_0 specific resistance at Δp = 1 MPa (m kg^{-1} MPa^{-n})
γ index in the consolidation coefficient equation (11)
δ constant in the consolidation behaviour index equation (12)
ε_s volume fraction of solids in the mixture
μ liquid viscosity (Pa s)
v consolidation behaviour index
ρ liquid density (kg m^3)
ρ_s true density of the particle (kg m^3)
ω_0 volume of solids in the press per unit area (m^3 m^{-2})

Subscript:
1 at the transition between the filtration and compression stages
∞ equilibrium value

REFERENCES

1. M. Shirato, T. Murase, E. Iritani, F.M. Tiller and A.F. Alciatore, in *Filtration*, M.J. Matteson and C. Orr (Eds.), Marcel Dekker, New York (1981).

2. R.J. Hunter, *The Zeta Potential in Colloid Science*, Academic Press, London (1981).

3. R.J. Hunter, *Foundations of Colloid Science*, Clarendon Press, Oxford (1987).

4. R.H. Ottewill, Direct measurements of particle-particle interactions, *Prog. Colloid & Polymer Science*, **57**, 71 (1980).

Cite paper as: Wakeman R.J., Tarleton E.S. and Sabri M.N., 1992, Effects of the solid-liquid interface in filter cake formation and consolidation, *Proc. European Symposium on Solid-Liquid Separation*, Paper L16, 14 pp., Cologne, Germany.

5. R.J. Wakeman, M.N. Sabri and E.S. Tarleton, Factors affecting the formation and properties of wet compacts, *Powder Technology*, **65**, 283-292, 1991.

6. S.T. Thuraisingham and R.J. Wakeman, A new approach to the study of the filtration of stable suspensions, *Proc. 20th Biennial Conf. of the International Briquetting Association*, pp.389-401, 1987.

7. M. Shirato, T. Murase and M. Iwata, in *Progress in Filtration and Separation: 4*, R.J. Wakeman (Ed.), Elsevier, Amsterdam (1986).

8. B. Sivaram and P.K. Swamee, *J. Japanese Soc. Soil Mech. Found. Eng.*, **17**, 48 (1977).

9. K. Terzaghi and P.B. Peck, *Soil Mechanics in Engineering Practice*, Wiley, New York (1948).

10. D.W. Taylor, *Fundamentals of Soil Mechanics*, *5th Edn.*, pp.225-229, Wiley, New York (1962).

Cite paper as: Wakeman R.J., Tarleton E.S. and Sabri M.N., 1992, Effects of the solid-liquid interface in filter cake formation and consolidation, *Proc. European Symposium on Solid-Liquid Separation*, Paper L16, 14 pp., Cologne, Germany.

FIGURES AND TABLES

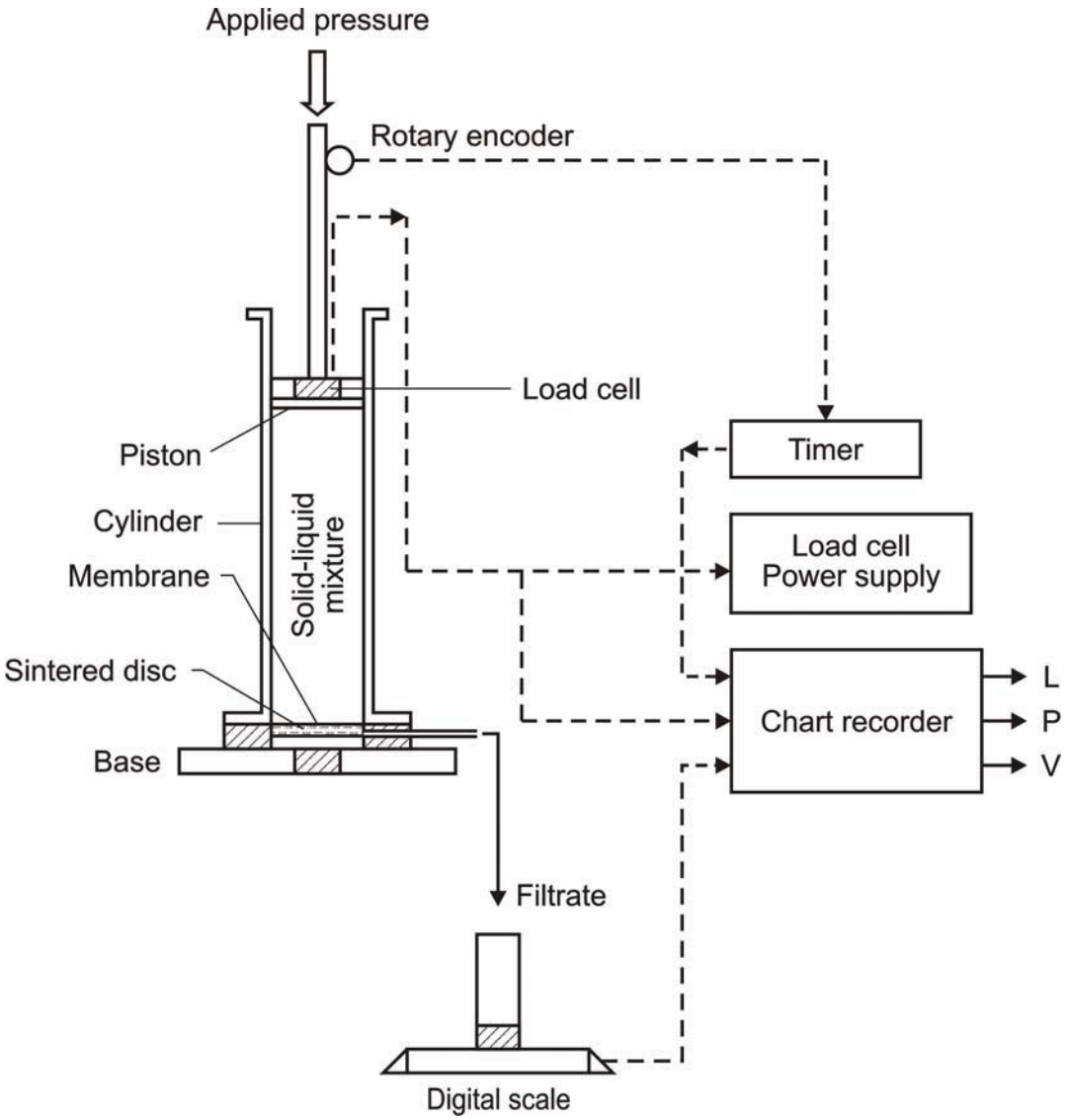

Figure 1: Line diagram of the experimental apparatus.

Cite paper as: Wakeman R.J., Tarleton E.S. and Sabri M.N., 1992, Effects of the solid-liquid interface in filter cake formation and consolidation, *Proc. European Symposium on Solid-Liquid Separation*, Paper L16, 14 pp., Cologne, Germany.

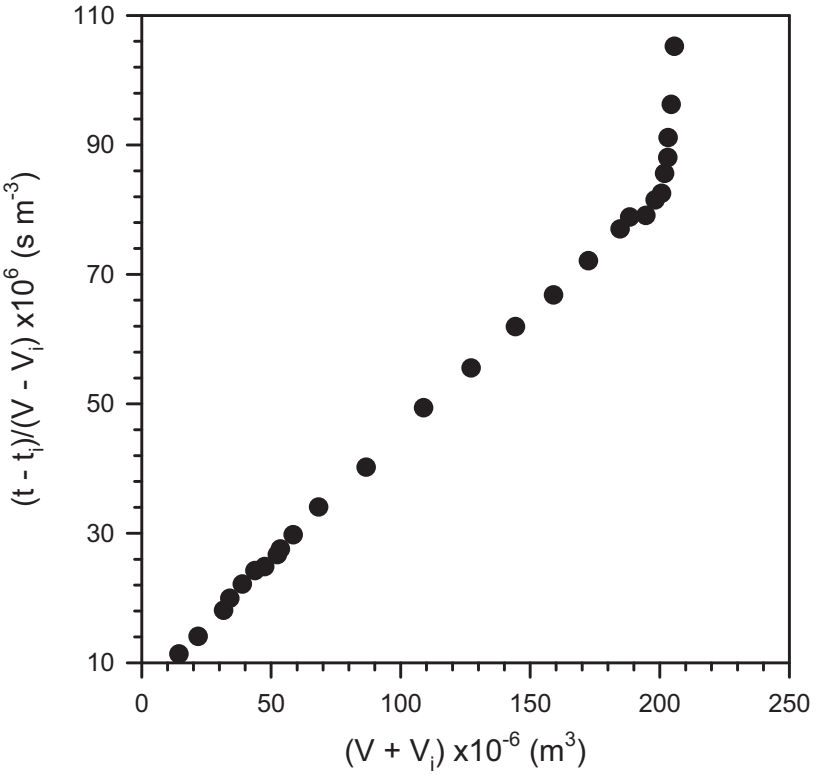

Figure 2: 'Filtration plot' of china clay experimental data (x_{av} = 3.3 μm, pH = 5.2, p = 6.4 MPa).

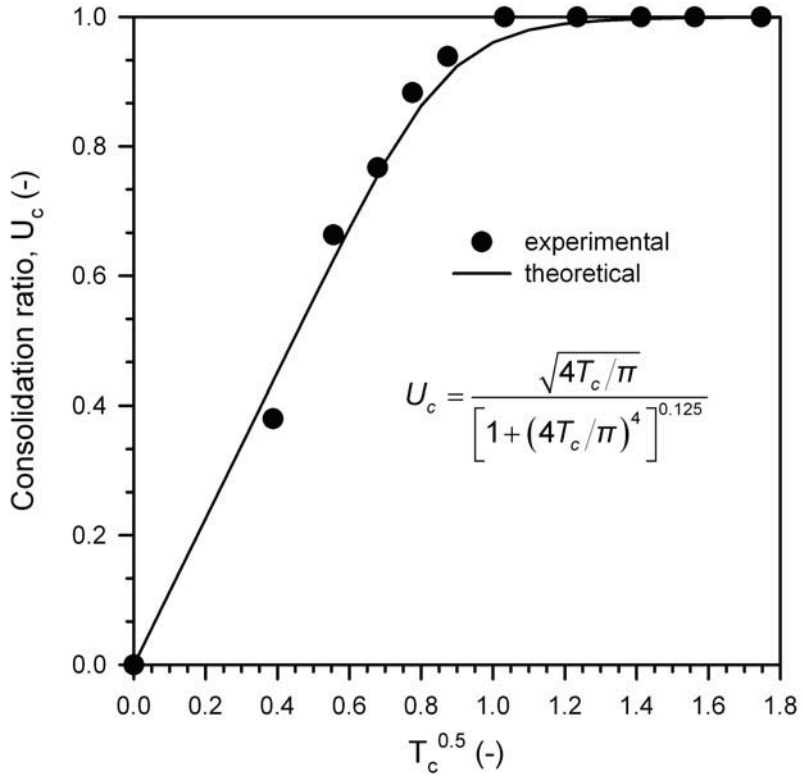

Figure 3: 'Consolidation plot' of china clay experimental data (x_{av} = 3.3 μm, pH = 5.2, p = 6.4 MPa).

Cite paper as: Wakeman R.J., Tarleton E.S. and Sabri M.N., 1992, Effects of the solid-liquid interface in filter cake formation and consolidation, *Proc. European Symposium on Solid-Liquid Separation*, Paper L16, 14 pp., Cologne, Germany.

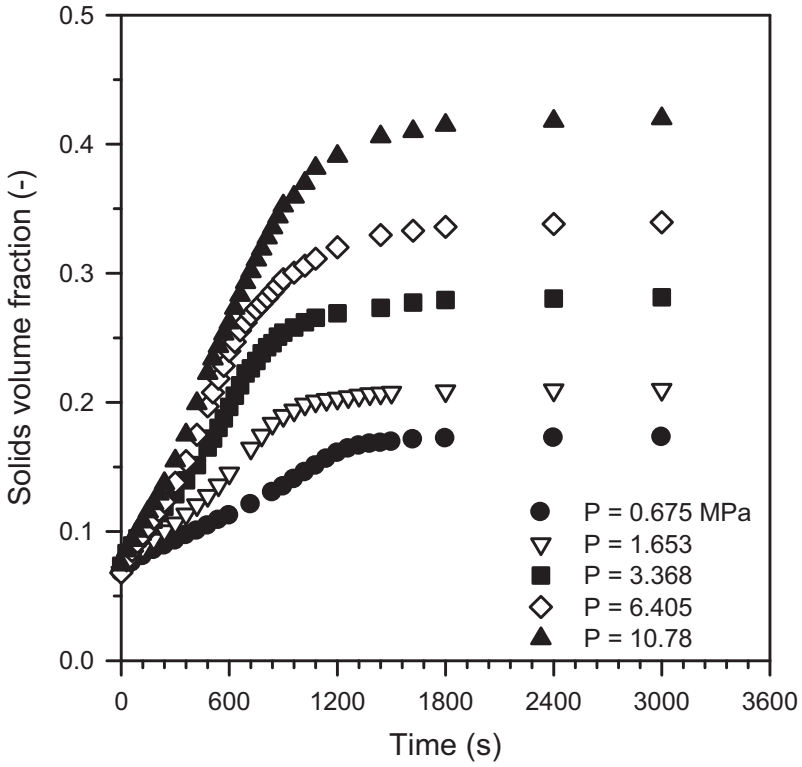

Figure 4: Effect of pressure on hydromagnesite suspension filtration (x_{av} = 16.4 μm, pH = 9.9).

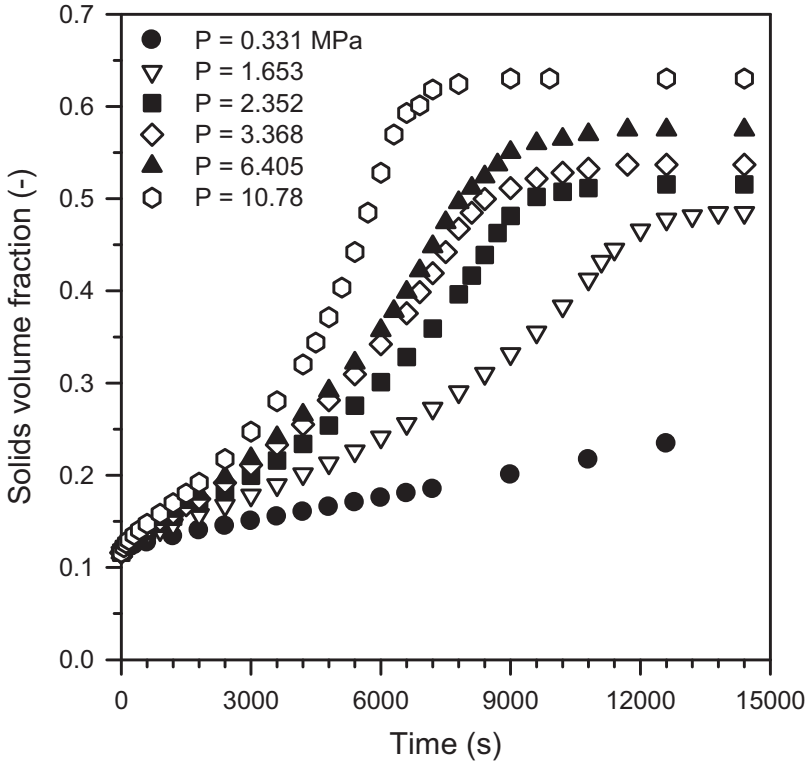

Figure 5: Effect of pressure on china clay suspension filtration (x_{av} = 5.4 μm, pH = 5.2).

Cite paper as: Wakeman R.J., Tarleton E.S. and Sabri M.N., 1992, Effects of the solid-liquid interface in filter cake formation and consolidation, *Proc. European Symposium on Solid-Liquid Separation*, Paper L16, 14 pp., Cologne, Germany.

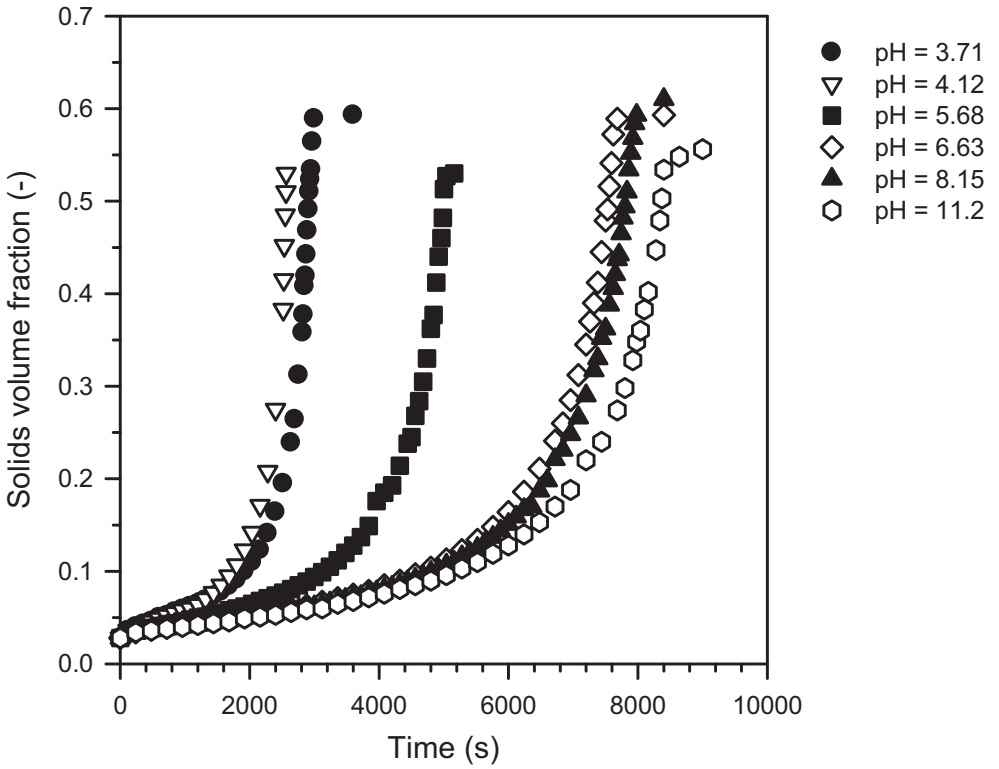

Figure 6: Effect of pH on unwashed anatase suspension filtration (x_{av} = 0.3 μm, isoelectric pH ≈ 4, p = 2.7 MPa).

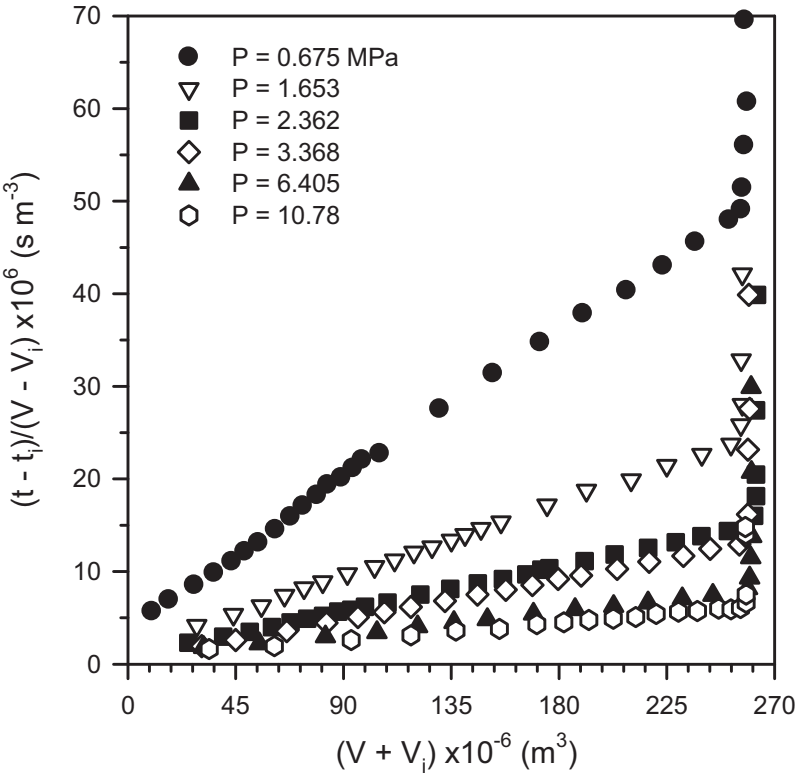

Figure 7: Effect of pressure on 'filtration plot' of anatase experimental data (x_{av} = 0.3 μm, pH = 4 (isoelectric point)).

Cite paper as: Wakeman R.J., Tarleton E.S. and Sabri M.N., 1992, Effects of the solid-liquid interface in filter cake formation and consolidation, *Proc. European Symposium on Solid-Liquid Separation*, Paper L16, 14 pp., Cologne, Germany.

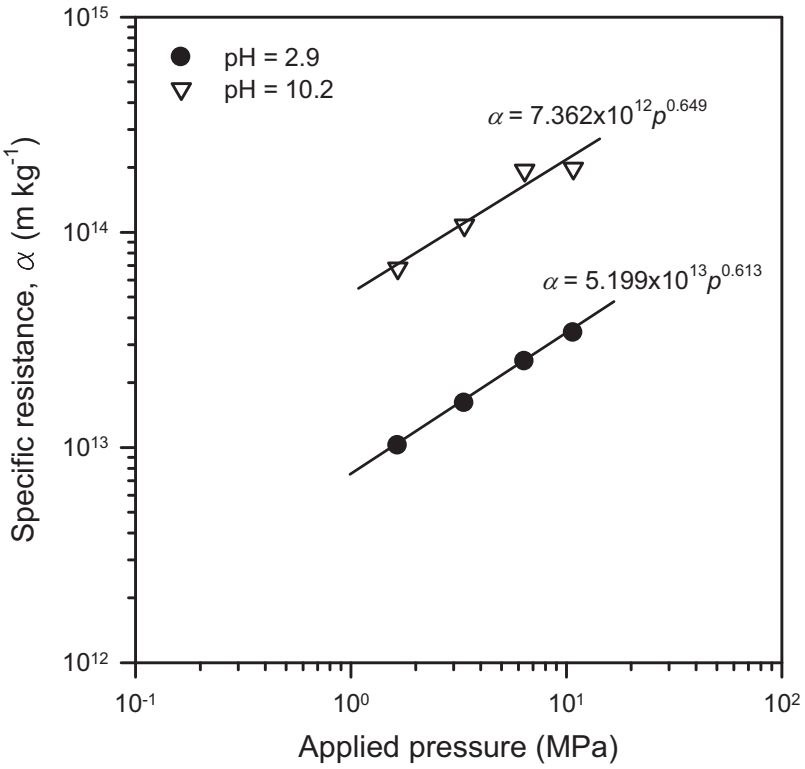

Figure 8: Dependence of specific resistance of china clay on pressure and pH (x_{av} = 3.3 µm).

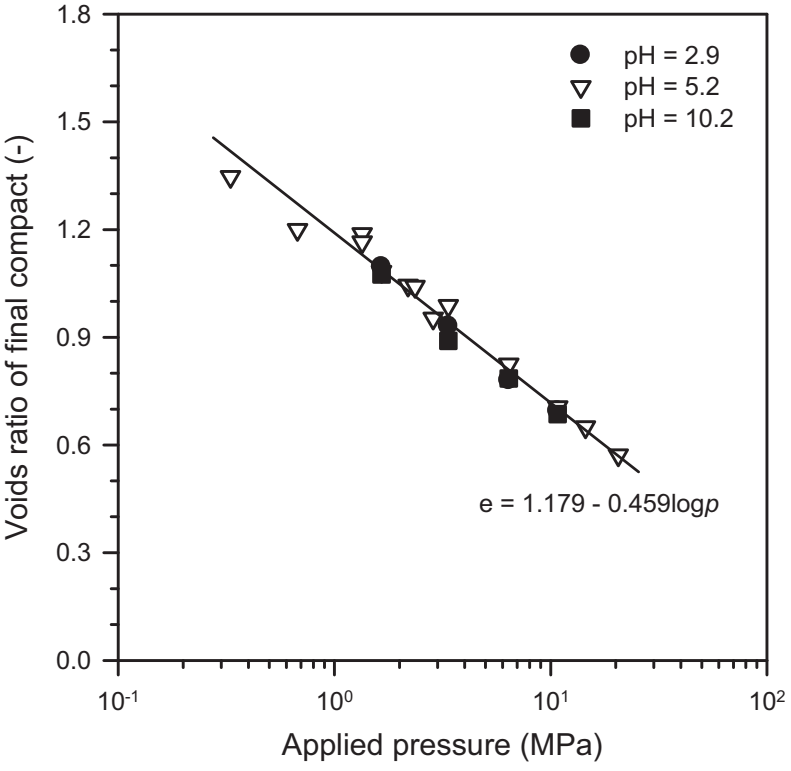

Figure 9: Dependence of ultimate voids ratio of china clay cakes on pressure and pH (x_{av} = 3.3 µm).

Cite paper as: Wakeman R.J., Tarleton E.S. and Sabri M.N., 1992, Effects of the solid-liquid interface in filter cake formation and consolidation, *Proc. European Symposium on Solid-Liquid Separation*, Paper L16, 14 pp., Cologne, Germany.

Particle	Mean size (μm)	Shape	Surface charge
Anatase	0.6	Tetragonal	High
Aragonite	1.7, 3.5, 8.2, 10	Elongated	Low
Calcite	3, 15	Rhomboidal	Low
China clay	1.3, 3.3, 5.4	Platelets	Medium-high
Hydromagnesite	16.4	Rhomboidal	Medium-low

Table 1: General characteristics of particles used in this study.

Particle type	pH	X_{av} (1)	α_0 (2)	n	e_0	b	C_{e0} (3)	γ	δ (4)
Anatase*	4.0	0.5	7.161×10^{11}	0.222	1.681	0.134	3.553×10^{-11}	0.915	0
	7.0	0.5	5.353×10^{12}	0.027	5.916	0.318	1.657×10^{-12}	1.093	0
	9.1	0.5	3.498×10^{12}	0.111	8.787	1.222	9.352×10^{-12}	0.912	0
Aragonite**	11.0	1.7	1.382×10^{11}	0.227	4.286	0.687	1.869×10^{-10}	1.098	
	11.0	3.5	4.795×10^{10}	0.214	4.722	0.812	3.924×10^{-9}	0.752	
	11.0	8.2	5.981×10^{9}	0.26	6.558	1.239	3.17×10^{-8}	0.546	
	11.0	10.0	5.567×10^{8}	0.551	8.704	1.825	5.450×10^{-8}	0.502	
Calcite***	9.2	3.0	8.346×10^{10}	0.246	4.951	0.619	7.605×10^{-10}	0.822	
China clay****	2.9	3.3	8.318×10^{10}	0.649	2.695	0.499	2.865×10^{-8}	0.168	0
	5.2	1.3	8.649×10^{10}	0.648	2.968	0.546	8.186×10^{-9}	0.263	0
	5.2	3.3	4.018×10^{11}	0.458	2.521	0.446	1.288×10^{-9}	0.533	0
	5.2	5.4	5.572×10^{10}	0.581	2.491	0.469	7.148×10^{-8}	0.116	0
†	5.2	floc			2.955	0.54			
	10.2	3.3	7.532×10^{11}	0.613	2.567	0.469	2.747×10^{-10}	0.499	0
††	3-10	3.3			2.556	0.459			
Hydromagnesite*	9.9	16.4	1.041×10^{10}	0.564	12.00	2.636	4.108×10^{-7}	-0.08	1.76

*Applied pressure range 300 to 11,000 kPa; **Applied pressure range 200 to 1000 kPa; ***Applied pressure range 130 to 2100 kPa; ****Applied pressure range 300 to 20,000 kPa
†Suspension flocculated by Magnafloc 351 (from Allied Colloids); ††Only the voids ratio data for all pH's form a common line
Units: (1) μm; (2) m kg^{-1} kPa^{-n}; (3) m^2 s^{-1} $kPa^{-\gamma}$; (4) kPa.

Table 2: Coefficients of the constitutive equations for the systems studied.

Cite paper as: Wakeman R.J., Tarleton E.S. and Sabri M.N., 1992, Effects of the solid-liquid interface in filter cake formation and consolidation, *Proc. European Symposium on Solid-Liquid Separation*, Paper L16, 14 pp., Cologne, Germany.